PERGAMON

Deep-Sea Research II 49 (2002) 107–121

DEEP-SEA RESEARCH
PART II

www.elsevier.com/locate/dsr2

Detecting *Trichodesmium* blooms in SeaWiFS imagery

Ajit Subramaniam[a,*], Christopher W. Brown[b], Raleigh R. Hood[c], Edward J. Carpenter[d], Douglas G. Capone[a]

[a] *Department of Biological Sciences and The Wrigley Institute for Environmental Studies, University of Southern California, Los Angeles, CA 90089, USA*
[b] *NOAA/NESDIS, E/RA3, 5200 Auth Road, Camp Springs, MD 20746, USA*
[c] *University of Maryland Center for Environmental Science, Cambridge, MD 21613, USA*
[d] *Romberg Tiburon Center, San Francisco State University, Tiburon, CA 94920, USA*

Accepted 12 June 2001

Abstract

A multispectral classification scheme was developed to detect the cyanobacteria *Trichodesmium* spp. in satellite data of the sea-viewing wide field-of-view sensor (SeaWiFS). The criteria for this scheme were established from spectral characteristics derived from (1) SeaWiFS imagery of a *Trichodesmium* bloom located in the South Atlantic Bight and (2) modeled remote sensing reflectances of *Trichodesmium* and other phytoplankton. The classification scheme, which is valid for moderate chlorophyll concentrations of *Trichodesmium* in coastal waters, is based on the magnitude of the 490-channel reflectance and the spectral shape of remote sensing reflectance at 443, 490 and 555 nm. Analysis suggests that the spatial structure of *Trichodesmium* populations at sub-pixel scales must be considered when employing spectral characteristics to detect their presence in satellite imagery. This study demonstrates the potential of mapping *Trichodesmium* from space using spectral observations, even in waters as optically complex as the South Atlantic Bight. Future efforts, which will incorporate ancillary data such as wind speeds and water temperature, will improve the likelihood of correct identification.

1. Introduction

The planktonic marine cyanobacterium *Trichodesmium* sp. is broadly distributed throughout the oligotrophic marine tropical and sub-tropical oceans (Capone and Carpenter, 1982; Capone et al., 1997). *Trichodesmium*, which typically occurs in macroscopic bundles or colonies, is

*Corresponding author.
E-mail address: ajits@rcf.usc.edu (A. Subramaniam).

PII: S0967-0645(01)00096-0

noteworthy for its ability to form large surface aggregations and to fix dinitrogen gas. The latter is important because primary production supported by N_2 fixation can result in a net export of carbon from surface waters to the deep ocean and play a significant role in the global carbon cycle (Hood et al., 2000). Information on the distribution and density of *Trichodesmium* is required to quantitatively estimate their contribution to global N_2 fixation on global and regional scales.

Unfortunately, information of the distribution pattern of *Trichodesmium* is very sparse and biased by shipboard measurements. As a result, present estimates of N_2 fixation by *Trichodesmium* are highly uncertain (Hood et al., 2000). In order to better constraint estimates of N_2 fixation by *Trichodesmium* and improve our understanding of their broader biogeochemical importance in the oceans, we need to define better their spatial and temporal variability on a global scale. One approach that holds great promise is satellite remote sensing. Satellite ocean color sensors, such as the sea-viewing wide field-of-view sensor (SeaWiFS; McClain et al., 1998), are ideal instruments for estimating global phytoplankton biomass, especially in episodic blooms, because they provide relatively high frequency synoptic information over large areas. *Trichodesmium* is well suited for identification from space because its population maximum is usually at 15–30 m and it has a combination of specific ultrastructure and biochemical features that result in a relatively unique spectral signature that should be detectable by ocean color sensors (Subramaniam et al., 1999b). These features include high backscatter due to the presence of gas vesicles and the absorption and fluorescence of its accessory pigment phycoerythrin.

Attempts to empirically develop a scheme to identify *Trichodesmium* in satellite imagery have been hindered by the absence of contemporaneous observations of documented blooms by satellites. As a result, previous efforts have relied heavily on optical modeling and laboratory optical measurements. An optical model developed by Subramaniam et al. (1999b) predicted that the magnitude of water-leaving radiances at 412 nm for *Trichodesmium* always should be lower than that of other phytoplankton due its higher chlorophyll-specific absorption, while the water-leaving radiance at 555 nm always should be higher for *Trichodesmium* than other phytoplankton due to the influence of phycoerthrin fluorescence. Subramaniam et al. (1999b), using modeled hyperspectral remote sensing reflectances, concluded that *Trichodesmium* was not distinguishable from other phytoplankton at concentrations less than about 1.0 mg Chl/m^3. The study also demonstrated that standard ocean color chlorophyll algorithms would underestimate *Trichodesmium*-specific chlorophyll by a factor of at least four due to self-shading by the colonies.

Trichodesmium routinely occurs, often in very dense surface aggregations, in the South Atlantic Bight, a region located off the southeastern coast of the United States from South Carolina to Florida (Hulbert, 1967; Marshall, 1971; Dunstan and Hosford, 1977). Dunstan and Hosford (1977) found *Trichodesmium* throughout the year in these waters, present in at least 36% of the sampled stations in December to 76% of the stations in July, and sometimes contributing over 50% of the particulate organic carbon at the surface (100–150 μg C/l). The densest concentrations usually were observed at midshelf stations located between the 20 and 200 m isobaths. In July 1974, a shelf-wide bloom with a maximum colony density of 36,000 trichomes/l (9 mg Chl/m^3 *Trichodesmium*-specific chlorophyll) was encountered (Dunstan and Hosford, 1977).

We present here the development and application of a multispectral classification scheme for detecting *Trichodesmium* in ocean color measurements. The scheme is based on spectral characteristics obtained from SeaWiFS imagery of a *Trichodesmium* bloom located in the South

Atlantic Bight and remote sensing reflectances of waters containing *Trichodesmium* and other phytoplankton calculated from an optical model.

2. Development of classification scheme

2.1. Optical modeling

Normalized water-leaving radiances (nLw(λ), where $\lambda = 412$, 443, 490, 510 and 555 nm) for *Trichodesmium* and other phytoplankton, were modeled for chlorophyll concentrations ranging from 0.5 to 10 mg Chl/m^3 using a remote sensing reflectance model similar to the one described by Subramaniam et al. (1999b). Remote-sensing reflectance, R_{rs}, is expressed as the ratio of upwelling radiance, L_u, to downwelling irradiance, E_d. The spectral model,

$$R_{rs}(\lambda) = \frac{L_u(\lambda)}{E_d(\lambda)} \cong 0.083 \frac{b_b(\lambda)}{a(\lambda)}, \quad (1)$$

where b_b and a are the coefficients of backscattering and absorption, was based on Monte Carlo modeling calculations appropriate for waters with a relatively broad range of scattering to absorption ratios (Kirk, 1994, Eq. (6.5)). The backscatter and absorption coefficients in Eq. (1) can be expressed as the sum of their individual components. Thus, backscattering is

$$b_b(\lambda) = b_{bw}(\lambda) + b^*_{bp}(\lambda)C + b^*_{bT}(\lambda)C + b^*_{bd}(\lambda)C, \quad (2)$$

where b_{bw} is the backscatter coefficient of water, b_{bp}* is the chlorophyll-specific backscatter due to phytoplankton; b_{bT}* is the chlorophyll-specific backscatter due to *Trichodesmium*; and b^*_{bd} is the chlorophyll-specific backscatter due to detrital material (Table 1).

Similarly, absorption is

$$a(\lambda) = a_w(\lambda) + a^*_p(\lambda)C + a^*_T(\lambda)C + a_{dg}(\lambda), \quad (3)$$

where a_w is the absorption coefficient of water, a_P* is the average of chlorophyll-specific absorption coefficients of nine different phytoplankton species representing four classes, a_T* is the

Table 1
The parameters used in the optical model are explained in detail in Ref. Subramaniam et al. (1999b)[a]

Parameter	Symbol	412 (nm)	443 (nm)	490 (nm)	510 (nm)	555 (nm)
Backscatter due to water	b_{bw}	0.0032	0.0025	0.0016	0.0013	0.0009
Backscatter due to phytoplankton and detritus	$b^*_{bp} + b_{bd}$	0.0046	0.0044	0.0040	0.0038	0.0036
Backscatter due to *Trichodesmium* and detritus	$b^*_{bT} + b_{bd}$	0.0049	0.0052	0.0061	0.0063	0.0074
Absorption due to water	a_w	0.0047	0.0064	0.0150	0.0325	0.0596
Chlorophyll-specific absorption of phytoplankton	a^*_p	0.0292	0.0309	0.0231	0.0168	0.0077
Chlorophyll-specific absorption of *Trichodesmium*	a^*_T	0.0523	0.0368	0.0288	0.0247	0.0132
Absorption of colored dissolved matter	a_{dg}	0.0471	0.0286	0.0105	0.0070	0.0029

[a] Values for B_{bw} are from Smith and Baker (1981) (1/2 b_w), for $b^*_{bp} + b_{bd}$, from Morel (1988), for $b^*_{bT} + b_{bd}$, from Subramaniam et al. (1999b), for a_w, from Pope and Fry (1997), a^*_p, from Sathyendranath et al. (1987), and a^*_T from Subramaniam et al. (1999a).

chlorophyll-specific absorption coefficient of *Trichodesmium*, and a_{dg} is absorption due to detrital matter (Table 1). To estimate a_{dg}, we used the exponential formulation of Bricaud et al. (1981) with coefficients appropriate for the South Atlantic Bight (Nelson and Guarda, 1995), such that

$$a_{dg}(\lambda) = a(\lambda_0)e^{-S(\lambda-\lambda_0)} = 0.05e^{-0.02(\lambda-412)}. \quad (4)$$

Combining Eqs. (2)–(4), the remote sensing reflectance can be estimated from

$$R_{rs}(\lambda) = 0.083\frac{(b_{bw}(\lambda) + b^*_{bp}(\lambda)C + b^*_{bT}(\lambda)C + 0.30C^{0.62}[0.02(0.5 - 0.25\log C)(550/\lambda)])}{(a_w(\lambda) + a^*_p(\lambda)C + a^*_T(\lambda)C + 0.05e^{-0.02(\lambda-412)})}. \quad (5)$$

The model was parameterized for five bands of 10 nm width matched to the SeaWiFS sensor, and remote sensing reflectance was converted to normalized water-leaving radiance (units: $mW/cm^2/\mu m/sr$) by multiplying R_{rs} by the wavelength appropriate extraterrestrial solar irradiance.

To compute the spectra for varying concentrations of *Trichodesmium* in the absence of other phytoplankton, the chlorophyll concentration of other phytoplankton was set to 0. Conversely, to compute the reflectance spectra for varying concentrations of "other phytoplankton", the chlorophyll concentration of *Trichodesmium* was set to 0. To study the effect of mixed populations, the reflectance spectra of a varying percentage of *Trichodesmium* to other phytoplankton for a total chlorophyll concentration of 1 mg Chl/m^3 was computed.

2.2. Empirical approach

In addition to the optical model, the spectral signature of a *Trichodesmium* bloom was determined empirically by extracting water-leaving radiances from a bright feature in a SeaWiFS image of the South Atlantic Bight from October 30, 1998, deemed to be a portion of a *Trichodesmium* bloom sampled on November 1, 1998.

2.2.1. South Atlantic Bight trichodesmium bloom

A cruise was conducted in the South Atlantic Bight (SAB) from October 27 to November 13, 1998. During the cruise, a *Trichodesmium* bloom was encountered and bucket samples were taken whenever *Trichodesmium* seemed visually abundant at the surface for enumeration. Counts were determined using an epifluorescence microscope. Thin surface accumulations of *Trichodesmium* were evident along the 200 m isobath while steaming south out of Beaufort, NC. On October 30, dense accumulations of *Trichodesmium* were encountered at the surface during a period of exceptionally calm weather in the morning. At 9:45 AM, the patch was a few meters wide but appeared many kilometers long, and a sample taken for cell counts contained 6700 trichomes/l (equivalent *Trichodesmium*-specific chlorophyll concentration = 1.68 mg Chl/m^3). Outside the patch, average chlorophyll concentrations were 0.37 mg Chl/m^3, about 1/5th of the calculated *Trichodesmium*-specific chlorophyll within the patch. These accumulations disappeared as wind speeds increased after 11:00 AM. On October 31, isolated accumulations of intermediate densities measuring a few meters wide were observed throughout the day along the shelf break. On November 1, a *Trichodesmium* bloom was seen as the ship steamed westward from the shelf break towards Jacksonville, FL. The bloom was arranged as a series of elongated patches, several 100 m in width, oriented in a north–south direction, turning the water greenish-yellow. A sample in the middle of a very large accumulation contained 12,300 trichomes/l, and *Trichodesmium*-specific chlorophyll (= 3.08 mg Chl/m^3) represented 71% of the total chlorophyll measured at this station. Twelve such patches were encountered over a period of 4 h and a distance of 60 km. After November 1, a low pressure system moved through the region accompanied by increased wind speeds, and no further surface accumulations of *Trichodesmium* were observed.

2.2.2. SeaWiFS imagery

High resolution picture transmission (HRPT) imagery of the South Atlantic Bight dating from October 25 to November 7, 1998 were obtained from the Goddard Distributed Active Archive Center and processed to normalized water-leaving radiance (nLw(λ), where $\lambda = 412$, 443, 490, 510 and 555 nm) and chlorophyll concentration using the SeaWiFS data analysis system (SeaDAS, version 3.3; Fu et al., 1998). Chlorophyll concentration was estimated using the default SeaDAS (OC2) algorithm (O'Reilly et al., 1998). *Trichodesmium*-specific chlorophyll was estimated by multiplying OC2 Chlorophyll by four to account for self-shading effects.

Preliminary examination of true-color SeaWiFS imagery indicated a highly reflective feature located along the continental shelf edge where the water depth ranged from 60 to 400 m and just inshore of the Gulf Stream. The feature was first observed in the October 27 image, centered at 28.5°N, 80.1°W. On October 30, it was seen centered at 29.1°N, 80.2°W. An image from October 30, 1998 (Fig. 1A) shows the *Trichodesmium* bloom (#1). Additional bright features also can be seen in the image, such as the northern edge of the Little Bahamas Bank (#2), the shallow and turbid waters off Cape Canaveral (#3), and along the coasts of Georgia (#4) and South Carolina (#5). On November 1, clouds and airplane contrails covered most of the region and it was difficult to distinguish between the reflective feature in the water and bright artifacts in the atmosphere. Remnants of the bright feature were observed in the image near 30°N, 80.3°W. This coincided with the location where the *Trichodesmium* bloom had been observed from ship that day, and confirms that this highly reflective feature was a *Trichodesmium* bloom. The image from 30 October was used for further analysis because it was the most cloud-free image of the six days.

Normalized water-leaving radiances and chlorophyll concentrations extracted along two orthogonal transects from this highly reflective feature in the SeaWiFS imagery of October 30 (Fig. 1B) are used in the development of the classification scheme described below. These measurements are considered to be representative of the *Trichodesmium* bloom sampled on November 1.

3. Results

3.1. Optical model

As expected, the spectral signature of *Trichodesmium* predicted by the optical model was different from that of other phytoplankton (Figs. 2A and B). At 0.5 mg Chl/m^3, while the shape of the spectra for *Trichodesmium* and other phytoplankton were similar, the model indicated that the magnitude of nLw(4 9 0), nLw(5 1 0) and nLw(5 5 5) was higher for *Trichodesmium*. This difference was accentuated at higher *Trichodesmium*-specific chlorophyll concentrations. In addition, for a

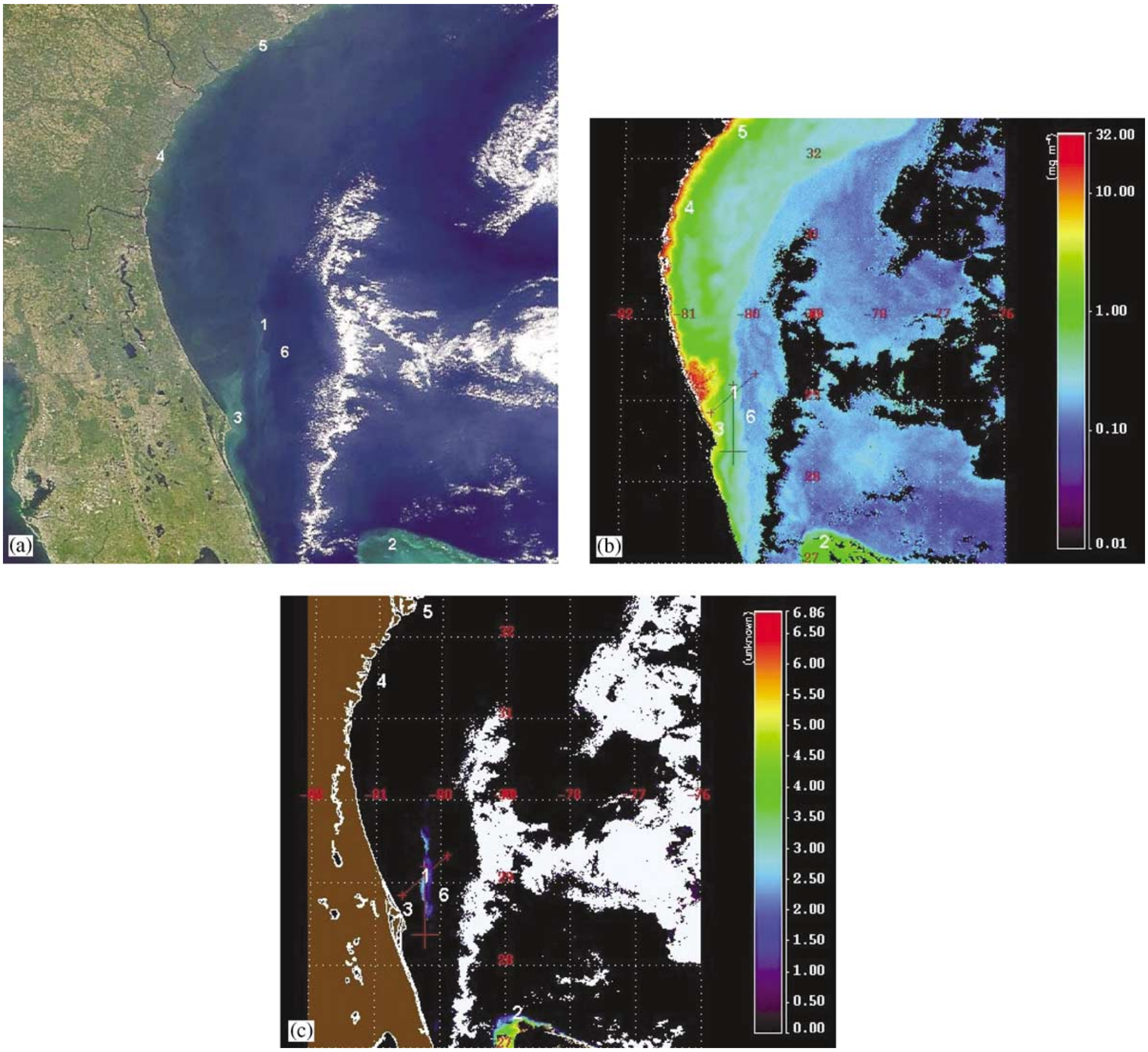

Fig. 1. SeaWiFS image of South Atlantic Bight from October, 30 1998. (A) True-color composite. (B) SeaWiFS-derived chlorophyll concentration. (C) *Trichodesmium*-specific chlorophyll concentration. Numbered features in A: (1) *Trichodesmium* bloom, (2) Little Bahamas Bank (water depth less than 8 m), (3) Cape Canaveral, (4) Georgia, (5) South Carolina, (6) Gulf Stream. The east–west and north–south transects plotted in Fig. 3A,B also are shown in B and C.

given chlorophyll concentration, the magnitude of nLw(5 5 5) was *always* higher for *Trichodesmium* than of other phytoplankton. At *Trichodesmium*-specific chlorophyll concentrations greater than 0.5 mg Chl/m^3, the magnitude of nLw(5 1 0) was greater than nLw(4 4 3). For *Trichodesmium*-specific chlorophyll concentrations between 0.5 and 1.5 mg Chl/m^3, the model predicted that nLw(4 9 0) should have the highest magnitude of all examined wavelengths. At concentrations of approximately 2 mg Chl/m^3 and greater, nLw(5 5 5) exceeded nLw(4 9 0).

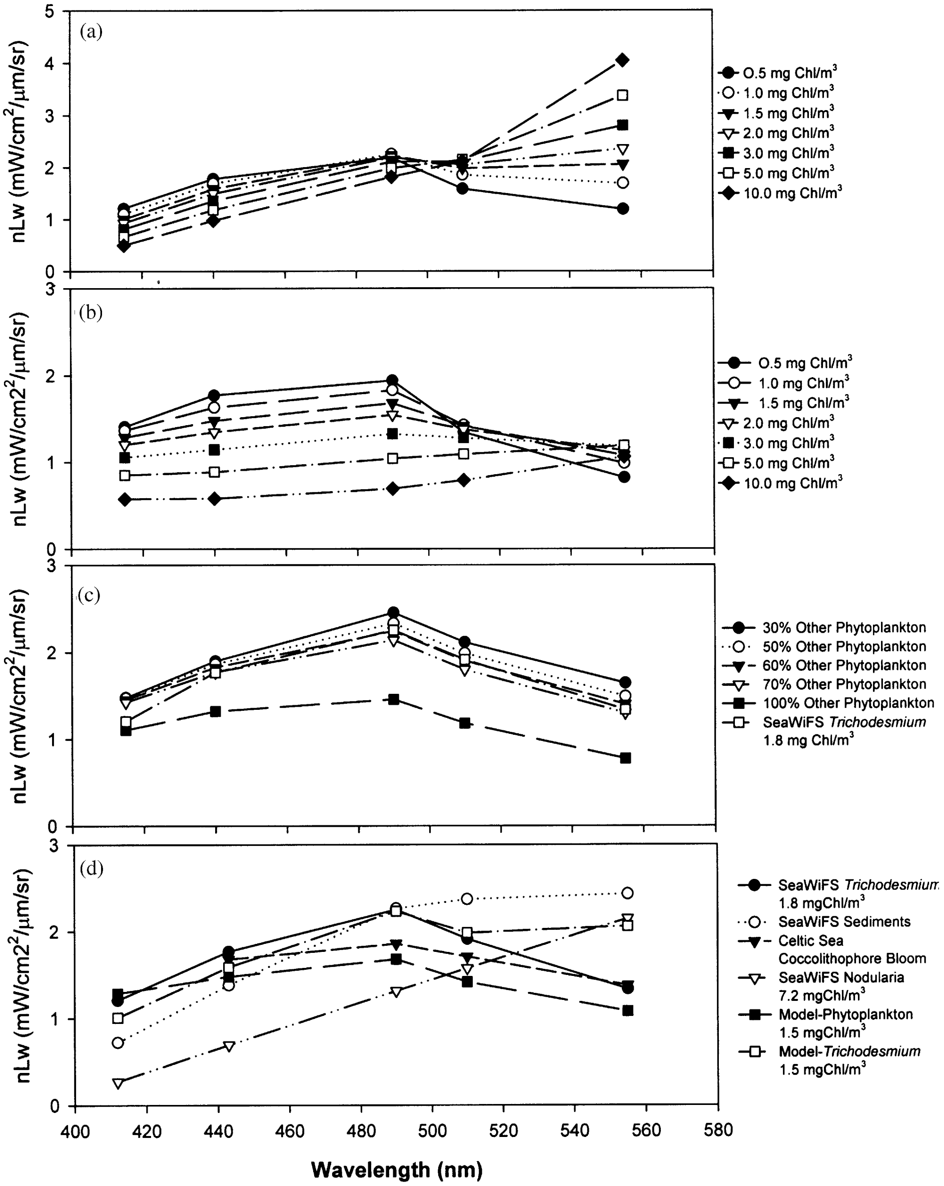

Fig. 2. Comparison of modeled and SeaWiFS derived spectra. Modeled water-leaving radiances of (A) *Trichodesmium* and (B) "other phytoplankton". Note difference in scale. (C) Modeled water-leaving radiances for varying proportions of other phytoplankton and *Trichodesmium* (total chlorophyll = 1 mg Chl/m^3). (D) Modeled and SeaWiFS derived water-leaving radiances of highly reflective oceanic phenomena. (SeaWiFS *Trichodesmium* and sediments spectra from image of October 30, 1998; SeaWiFS *Nodularia* spectrum from image of July 29 1999; Coccolithophore bloom spectrum from Brown and Yoder, 1994).

Mixing populations of other phytoplankton and *Trichodesmium* provided spectral characteristics intermediate between these two spectral end members. In particular, as the concentration of other phytoplankton increased, reflectance at 490 nm decreased and the spectral shape flattened (Fig. 2C).

3.2. Empirical results

The spectral difference between the highly reflective waters, with elevated *Trichodesmium* concentrations, and adjacent regions was also evident in the transects of nLw(λ) extracted from the October 30, 1998 SeaWiFS image of the SAB (Figs. 1B,C, and 3A,B). In the east–west transect, regions of *Trichodesmium* (at distances 29–43 km; also denoted by horizontal lines) exhibited elevated water-leaving radiances in all bands relative to clear waters of the Gulf Stream (0–28 km) and inner shelf waters (45–65 km; Fig. 3A). Also note that the increases were wavelength dependent; within the *Trichodesmium* bloom, nLw(4 9 0) achieved the highest values, followed by nLw(4 4 3) and nLw(5 1 0). In the shallow, turbid waters off Cape Canaveral (65–84 km), radiances also increased. The spectral dependence of this increase, however, differed from that found within the *Trichodesmium* region. Specifically, nLw(4 9 0), nLw(5 1 0), and nLw(5 5 5) increased almost uniformly, with nLw(5 5 5) reaching highest values, followed closely by nLw(5 1 0), nLw(4 9 0), and nLw(4 4 3).

These spectral differences were also apparent in the normalized water-leaving radiances extracted along the north–south transect, but were not as dramatic (Figs. 1B,C, and 3A,B). Because the majority of the transect remained within the confines of the bloom, the observed variability in spectra was likely due to the gradual decrease in concentration of *Trichodesmium* encountered from north to south in the transect.

The OC2-derived chlorophyll concentrations within the *Trichodesmium* region ranged from 0.15 to 0.65 resulting in a *Trichodesmium*-specific chlorophyll concentration of 0.5 to 3 mg Chl*a*/m^3. As can be seen in Figs. 3A and B, the bloom consistently possessed nLw(4 9 0) at values greater than 1.3 mW/cm^{-2}/μm/sr, and this was consequently employed as a criterion in the classification scheme. However, other conditions, specifically shallow, turbid waters, also were characterized by high nLw(4 9 0) values, and additional criteria were necessary to separate these two conditions. It was determined that the spectra shape—[nLw(4 9 0)−nLw(4 4 3)]/[nLw(4 9 0)−nLw(5 5 5)]—best delineated the *Trichodesmium* bloom from suspended sediments and other phytoplankton.

3.3. Comparison between empirical and model results

In general, the empirically determined spectral reflectances matched those estimated using the optical model. In a comparison between the spectral characteristics of *Trichodesmium* derived using both approaches (Fig. 2D), the values of nLw(4 9 0) and nLw(5 1 0) were the same. However, the empirically derived values of nLw(4 1 2) and nLw(5 5 5) were lower than predicted by the model, with the difference of nLw(5 5 5) being quite large. Also, while the empirical results indicated that the magnitude of nLw(5 1 0) and nLw(4 4 3) were almost the same, the model predicted that nLw(5 1 0) should be greater than nLw(4 4 3) for *Trichodesmium*.

The differences between results derived from the two approaches, however, were minor compared to the differences in the spectral signature of *Trichodesmium* and other phytoplankton (at comparable concentration) and other highly reflective phenomena, such as sediments and coccolithphore blooms (Fig. 2D).

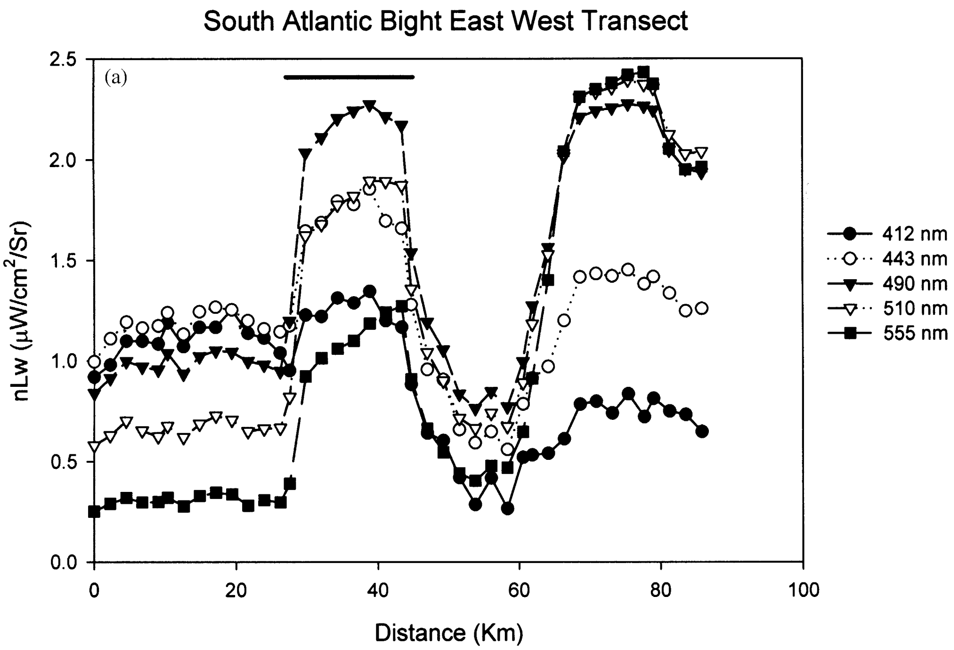

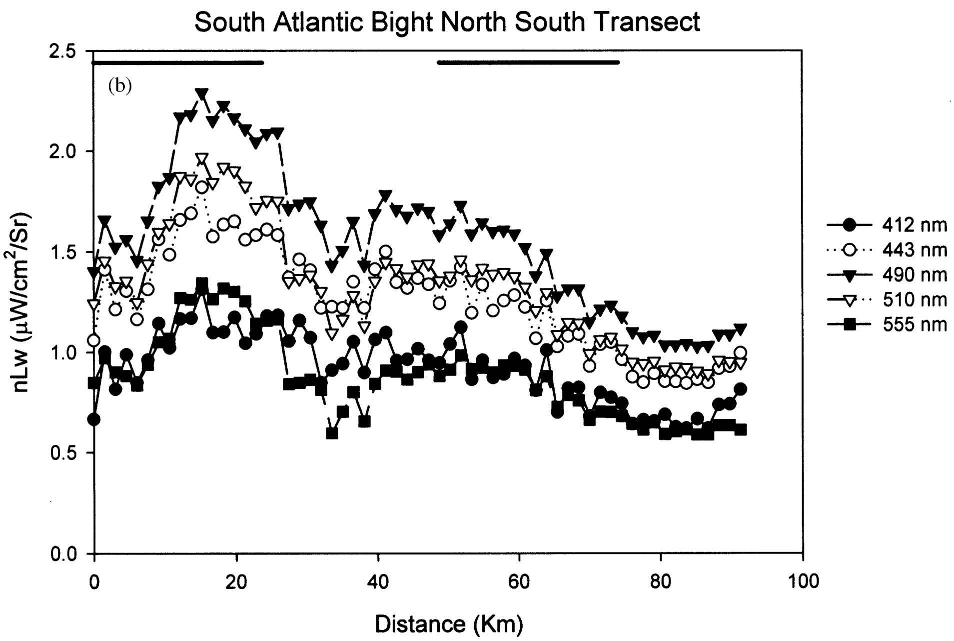

Fig. 3. Water-leaving radiances and chlorophyll concentration extracted from the SeaWiFS image of October 30, 1998 along the (A) east–west transect, and (B) north–south transect shown in Fig. 1B and C. The portion of the transect running through the *Trichodesmium* bloom is indicated by a bar.

3.4. Classification scheme

Based upon these empirical observations and model results, we propose the following classification scheme to identify the presence of *Trichodesmium* at moderate chlorophyll concentrations (0.5–3.0 mg/m^3) in SeaWiFS imagery: A pixel was flagged as dominated by *Trichodesmium* if the following three criteria were satisfied:

1. nLw(4 9 0) > 1.3 mW cm^2/μm/sr and nLw(4 9 0) > nLw(4 1 2), nLw(4 4 3), nLw(5 5 5)
2. nLw(5 1 0) > nLw443
3. 0.4 < [nLw(4 9 0)−nLw(4 4 3)]/[nLw(4 9 0)−nLw(5 5 5)] < 0.6

Criteria #1 and #2 represent absolute and relative magnitude thresholds, while criterion #3 depends on spectral shape. The threshold for nLw(4 9 0) was employed because it was a characteristic of *Trichodesmium* derived from both modeling and empirical results. The second criterion was selected from model results as a spectral characteristic unique to *Trichodesmium*. The shape factor was incorporated into the classification scheme to distinguish spectrally *Trichodesmium* from other phytoplankton and suspended sediments.

3.5. Application of classification scheme

The classification scheme was applied to the time-series of SeaWiFS imagery of the South Atlantic Bight from October 25 to November 7, 1998. In addition to the spectral criteria, a bathymetric (> 30 m) threshold also was applied to exclude high water-leaving radiance due to bottom reflectance from shallow waters, and certain combinations of sediments and colored dissolved organic matter that can mimic the reflectance pattern of a *Trichodesmium*. The bloom did not appear in the imagery until October 27, and no clear scenes were available after November 1. The classified *Trichodesmium* bloom appears as a spatially coherent feature that persisted in the imagery from October 27 to November 1 (Fig. 4). The *Trichodesmium*-specific chlorophyll concentration ranged from 0.5 to 3.0 mgChla/m^3, with a slight westward intensification. The *Trichodesmium* bloom evident in the image of October 27 centered at 28.5°N, 80.1°W appeared to lengthen and move northward on October 28. It was clearly evident in the image of October 30 centered at 29.1°N, 80.2°W (Fig. 1C). Remnants of the bloom were observed at 30°N, 80.3°W, coinciding with one of the locations of the *Trichodesmium* bloom observed from the ship that day. Note that the false positive response in the vicinity of the Little Bahamas Bank is likely due to incorrect bathymetric data.

4. Discussion

4.1. Optical model

The model that we present was parameterized for five bands of 10 nm width matched to the SeaWiFS sensor. The lack of spectral resolution of this model compared to the hyperspectral approach used by Subramaniam et al. (1999b) results in the loss of the reflectance peaks at 470 and 530 nm and the trough near 510 nm. Nonetheless, the combined results presented here show

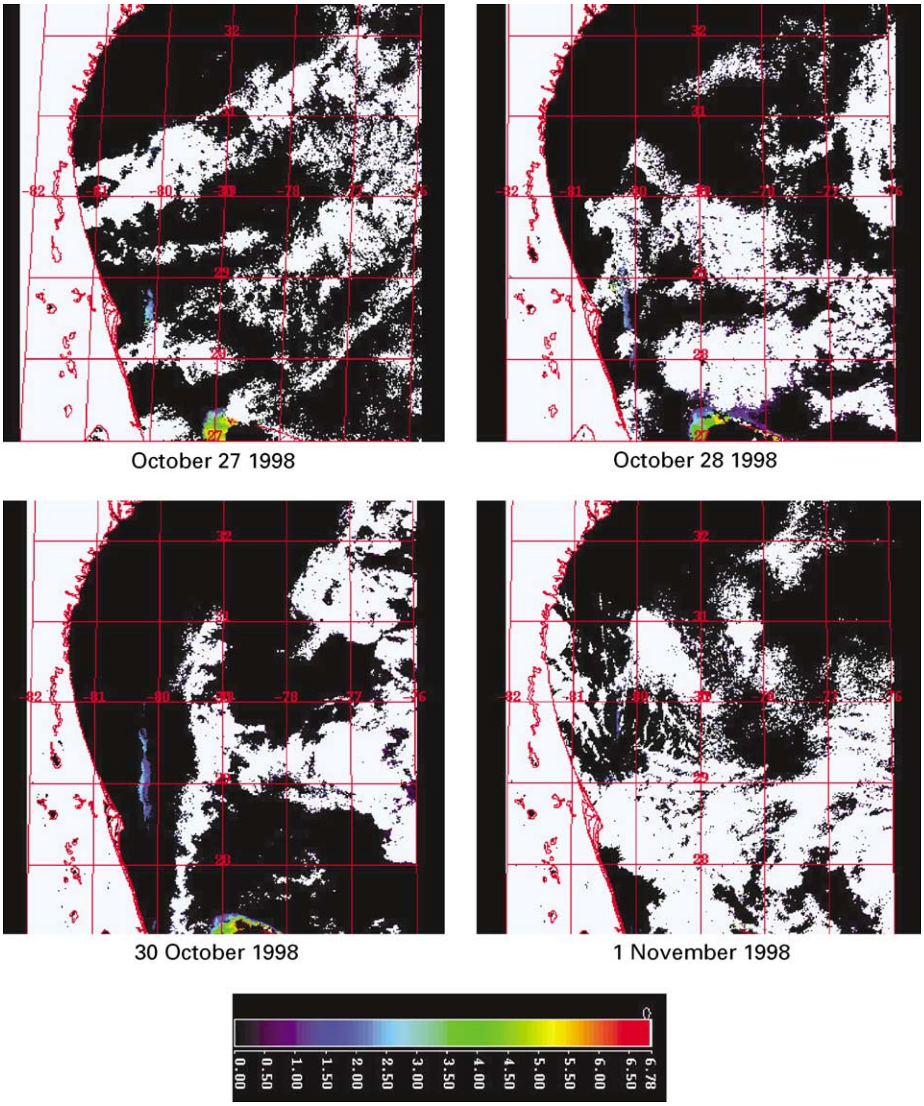

Fig. 4. *Trichodesmium*-specific chlorophyll as mapped by the classification scheme for SeaWiFS images from October 27 to November 1.

that moderate *Trichodesmium* concentrations can be detected remotely by SeaWiFs, even in optically complicated coastal waters. Other differences between the model of Subramaniam et al. (1999b) and the one presented here include a different parameterization of sky reflectance and detrial absorption, and calculation of the effect of mixed phytoplankton population on remote sensing reflectance. The present model can be improved in the way backscatter of detrital matter is parameterized. We have used the model of Morel (1988), which allows the backscatter of detrital matter to vary inversely with chlorophyll concentration. However, this was developed for Case I waters and may not be appropriate for coastal waters, especially when *Trichodesmium* or resuspended sediments are present.

A comparison of the model predicted and satellite-derived normalized water-leaving radiances indicates that the model over-predicts nLw(555). This could be because the model exaggerates the contribution of phycoerythrin fluorescence at chlorophyll concentrations of 1–2 mg chl/m^3. The backscatter + fluorescence spectra measurements detailed in Subramaniam et al. (1999b) were made on a concentrated collection of colonies in a small volume (about 20 colonies/ml) and equivalent to 100 mg Chl/m^3 of *Trichodesmium* chlorophyll. The fluorescence observed at such high concentrations may not be linearly scalable to lower chlorophyll concentrations between 0.5 and 2 mg Chl/m^3. However, it should be noted that the hyperspectral model of Subramaniam et al. (1999b) corresponded quite well in shape and magnitude with field measurements of a *Trichodesmium* bloom in the Caribbean Sea (Navarro Rodriguez, 1998).

4.2. Image classification

The use of SeaWiFS imagery in the development of a classification scheme for remote detection of *Trichodesmium* overcomes two problems of using a purely theoretical approach. The first problem is deriving the correct normalized water-leaving radiance from the satellite sensor measurement of total radiance. Inappropriate atmospheric correction has resulted in an underestimation of water-leaving radiance, even "negative" water-leaving radiance in coastal waters (Arnone, pers. Commun.; Stumpf, pers. Commun.; Siegel et al., 2000). Waters containing significant accumulations of *Trichodesmium* have a significant water-leaving radiance in the red and near infrared, which also can lead to errors in the atmospheric correction and underestimation of the water-leaving radiance in the blue and green bands of SeaWiFS. Developing a scheme based upon the measured radiances circumvents at least some of these kinds of problems because it results in criteria that take into account some of the potential errors in the atmospheric correction. Surface cyanobacterial blooms in the Baltic Sea have been observed with enough signal at 865 nm that portions of the bloom were misidentified as clouds (Subramaniam et al., 2000). Thus, high concentrations of *Trichodesmium* actually may be masked as clouds as might have happened in parts of the November 1 image.

The second problem that the empirical approach overcomes is that of mixed populations. As seen at the station occupied on November 1 in the South Atlantic Bight, even during a significant *Trichodesmium* accumulation with 12,700 trichomes/l, *Trichodesmium* only contributed 71% of the total chlorophyll in that bucket sample. Thus, even at relatively small scales when *Trichodesmium* abundances are high, the populations are mixed. Moreover, unlike most other phytoplankton that have homogeneous horizontal distributions in the near-surface water column, buoyant cyanobacteria such as *Trichodesmium* can be very patchy. Even in cases of very dense, nearly monospecific blooms, the satellite will likely see a mixture of *Trichodesmium* and other phytoplankton species because a SeaWiFS pixel is 1 km^2 while *Trichodesmium* blooms tend to occur in linear patches or striated patterns with width scales of 10s of m. Consequently, reflectance values for a pixel will usually be composed of a combination of characteristics of *Trichodesmium*, other phytoplankton, and clear water, and these three signals may not be separable by linear methods or simple band ratio type algorithms. In the empirical classification approach outlined above, we cannot mechanistically account for atmospheric correction or subpixel variability, but these are embedded into the data used.

4.3. Potential sources of error

There are other highly reflective conditions within oceanic and coastal waters that may possess the high backscattering characteristics of *Trichodesmium*. Such conditions include blooms of the coccolithophorids *Emiliania huxleyi* (Brown and Yoder, 1994) and *Geophyrocapsa oceanica* (Blackburn and Cresswell, 1993), the prymnesiophyte *Phaeocystis*, high concentrations of certain diatom species, and near-surface suspensions of sediments, as well as other cyanobacteria. For example, *Nodularia* possesses optical properties very similar to *Trichodesmium*. Some of these highly reflective phenomena are sufficiently spectrally different from *Trichodesmium* blooms to be clearly differentiated. For example, coccolithophorid blooms are milky blue in color while *Trichodesmium* blooms are generally greenish-yellow (Fig. 2D).

Phaeocystis and some diatom blooms, however, can be highly reflective and often contain sufficient quantities of photoprotectant pigments in the 470–510 nm range to mimic the spectral shape of *Trichodesmium*. In these cases, optical properties alone may be inadequate to distinguish *Trichodesmium*, and additional information will be required. For instance, because diatoms and *Phaeocystis* occupy a different ecological niche than does *Trichodesmium,* ancillary data such as water temperature and wind speed can be used to eliminate them from positive retrievals. *Trichodesmium* is mostly found at water temperatures greater than 25°C, while *Phaeocystis* and diatom blooms are more likely in colder waters of high latitudes or upwelling regions. Similarly, because *Nodularia*, is a brackish water species, not found in oligotrophic tropical oceans, it can be distinguished from *Trichodesmium* with salinity or geography. Bottom reflection from shallow coral reefs such as the Little Bahamas Bank also appears to satisfy the classification criteria as it too shows up in the classified image (Fig. 4). A simple depth criterion can be used to mask bottom reflection.

5. Conclusions

Trichodesmium is an organism with a unique combination of absorption, scattering and fluorescence properties that permit it to be spectrally identified in satellite ocean color imagery. In this paper, we have demonstrated that it is possible to identify *Trichodesmium* when it is present in sufficient quantities, even in optically complex coastal waters rich in CDOM and sediments. The classification scheme presented here detects only moderate concentrations of *Trichodesmium*. Even at these concentrations, the nitrogen fixed by *Trichodesmium* makes a very significant contribution to the nutrient budgets in some regions such as the Caribbean (Subramaniam, 1995). We did not find many pixels with the highly reflective signature of monospecific *Trichodesmium* predicted by the model. This is likely due to the spatial patchiness of *Trichodesmium* blooms in nature. We speculate that many of the classified *Trichodesmium* pixels contain a mixture of dense surface aggregations of *Trichodesmium* and intervening water, with the net response mimicking the signal generated by a lower concentration of *Trichodesmium*.

Although the semi-empirical nature of the classification scheme may restrict its application to coastal waters, the approach has the advantage of minimizing the impacts of errors in atmospheric correction, and it helps to overcome the confounding effects of patchiness and mixed *Trichodesmium*/phytoplankton populations. The present classification scheme is tuned to mixed populations in coastal waters where other phytoplankton and CDOM make a more significant contribution to the optical signal than would likely be found in a *Trichodesmium* bloom in the middle of the ocean. On the other hand, the scheme also is based on results derived analytically, and should function, at least to some degree, in coastal waters outside the South Atlantic Bight. To test quantitatively the scheme's robustness, increase its detection range, and modify it for use in a wide variety of oceanic environments, additional contemporaneous measurements of *Trichodesmium* concentrations, in situ water-leaving radiances, and satellite ocean-color imagery are needed.

Acknowledgements

A NASA SIMBIOS contract (NAS5-97131) to DGC, a NOAA Ocean Remote Sensing grant to CWB, and a NASA SMP grant to RRH, DGC and AS funded this work. We thank Pat Tester for the invitation to participate in the cruise and Mary Culver for help with the cruise logistics and encouragement all along. Ship time was obtained as a piggyback on a NAVO cruise and we thank the Chief Scientist Dennis Krynen, the Master and crew of the R/V Cape Hatteras for their assistance. We are especially grateful to Elin Haugan for assistance during the cruise and for counting the *Trichodesmium* samples. The authors would like to thank Norman Kuring for the true color images, the SeaWiFS Project (Code 970.2) and the Distributed Active Archive Center (Code 902) at the Goddard Space Flight Center, Greenbelt, MD 20771, for the production and distribution of the SeaWiFS data, respectively. These activities are sponsored by NASA's Mission to Planet Earth Program.

References

Bricaud, A., Morel, A., Prieur, L., 1981. Absorption by dissolved organic matter of the sea (yellow substance) in the UV and visible domains. Limnology and Oceanography 26, 45–53.

Blackburn, S.I., Cresswell, G., 1993. A coccolithophorid bloom in Jervis Bay, Australia. Australian Journal of Marine and Freshwater Research 44, 253–260.

Brown, C.W., Yoder, J.A., 1994. Coccolithophorid blooms in the global ocean. Journal of Geophysical Research 99, 7467–7482.

Capone, D.G., Carpenter, E.J., 1982. Nitrogen fixation in the marine environment. Science 217, 1140–1142.

Capone, D.G., Zehr, J.P., Paerl, H.W., Bergman, B., Carpenter, E.J., 1997. *Trichodesmium*, a globally significant marine cyanobacterium. Science 276, 1221–1229.

Dunstan, W.M., Hosford, J., 1977. The distribution of planktonic blue green algae related to the hydrography of the georgia bight. Bulletin of Marine Science 27, 824–829.

Fu, G., Baith, K.S., McClain, C.R., 1998. SeaDAS: The SeaWiFS data analysis system, Proceedings of The Fourth Pacific Ocean Remote Sensing Conference, Qingdao, China, July 28–31, 1998, pp. 73–79.

Hood, R.R., Michaels, A.F., Capone, D.G., 2000. Answers sought to the enigma of marine nitrogen fixation. EOS 81, 138–139.

Hulbert, E.M., 1967. Some notes on the phytoplankton of the southeastern coast of the United States. Bulletin of Marine Science 17, 330–337.

Kirk, J.T.O., 1994. Light and Photosynthesis in Aquatic Ecosystems, 2nd Edition. University Press, Cambridge, 509pp.

Marshall, H.G., 1971. Composition of phytoplankton off the southeastern coast of the United States. Bulletin of Marine Science 21, 806–825.

McClain, C.R., Cleave, M.L., Feldman, G.C., Gregg, W.W., Hooker, S.B., Kuring, N., 1998. Science quality SeaWiFS data for global biosphere research. Sea Technology September, 10–16.

Morel, A., 1988. Optical modeling of the upper ocean in relation to its biogenous matter content (case 1 water). Journal of Geophysical Research 93, 10–10,768.

Navarro Rodriguez, A.J., 1998. Optical properties of photosynthetic pigments and abundance of the cyanobacterium *Trichodesmium* in the Eastern Caribbean Basin. Ph.D. Thesis, University of Puerto Rico, Mayaguez, Puerto Rico.

Nelson, J.R., Guarda, S., 1995. Particulate and dissolved spectral absorption on the continental shelf of the southeastern United States. Journal of Geophysical Research 100, 8715–8732.

O'Reilly, J.E., Maritorena, S., Mitchell, B.G., Siegel, D.A., Carder, K.L., Garver, S.A., Kahru, M., McClain, C.R., 1998. Ocean color chlorophyll algorithms for SeaWiFS. Journal of Geophysical Research 103, 24–24,953.

Pope, R.M., Fry, E.S., 1997. Absorption spectrum (300–700 nm) of pure water: II integrating cavity measurements. Applied Optics 36, 8710–8723.

Sathyendranath, S., Lazzara, L., Prieur, L., 1987. Variations in the spectral values of specific absorption of phytoplankton. Limnology and Oceanography 32, 403–415.

Siegel, D.A., Wang, M., Maritorena, S., Robinson, W., 2000. Atmospheric correction of satellite ocean color imagery: The black pixel assumption. Applied Optics 39, 3582–3591.

Smith, R.C., Baker, K.S., 1981. Optical properties of the clearest natural waters (200–800 nm). Applied Optics 20, 177–184.

Subramaniam, A., 1995. Optical properties of the marine cyanobacterium *Trichodemsium* and their applications to remote sensing. Ph.D. Thesis, Marine Sciences Research Center. Stony Brook, State University of New York. 180pp.

Subramaniam, A., Carpenter, E.J., Karentz, D., Falkowski, P.G., 1999a. Optical properties of the marine diazotrophic cyanobacteria *Trichodesmium* spp.; I—absorption and spectral photosynthetic characteristics. Limnology and Oceanography 44, 608–617.

Subramaniam, A., Carpenter, E.J., Falkowski, P.G., 1999b. Optical properties of the marine diazotrophic cyanobacteria *Trichodesmium* spp.; II—a reflectance model for remote-sensing. Limnology and Oceanography 44, 618–627.

Subramaniam, A., Kratzer, S., Carpenter, E.J., Söderbäck, E., 2000. Remote sensing and optical in-water measurements of a cyanobacteria bloom in the Baltic Sea. Proceedings of the Sixth International Conference on Remote Sensing for Marine and Coastal Environments, Charleston, SC, Veridian ERIM International Vol. I, pp. 57–64.